POLITECNICO DI TORINO
Repository ISTITUZIONALE

Preliminary results on the timing response of CMOS LGADs for the ALICE 3 experiment

Original
Preliminary results on the timing response of CMOS LGADs for the ALICE 3 experiment / Fabbri, G., Bregant, M., Bufalino, S., Buthelezi, Z., Carnesecchi, F., Cavazza, D., Colocci, M., Corradino, T., Da Rocha Rolo, M., Durando, S., Endrizzi, J., Ferrero, C., Foertsch, S., Follo, U., Gioachin, G., Goodhead, J., Grenno, M., Iizuka, H., Lim, B., Di Nicolantonio, G., et al.. - In: JOURNAL OF INSTRUMENTATION. - ISSN 1748-0221. - 21:(2026). (21st Trento Workshop on Advanced Silicon Radiation Detectors (TREDI 2026) Perugia (Italy) 17–19 February 2026) [10.1088/1748-0221/21/08/c08022].
Availability:
This version is available at: 11583/3015867 since: 2026-09-24T07:35:59Z

Publisher:
Institute of Physics

Published
DOI:10.1088/1748-0221/21/08/c08022

Terms of use:

This article is made available under terms and conditions as specified in the corresponding bibliographic description in the repository

Publisher copyright

(Article begins on next page)

26 October 2026

Journal of
Instrumentation

OPEN ACCESS

Preliminary results on the timing response of CMOS LGADs for the ALICE 3 experiment

To cite this article: Gaia Fabbri *et al* 2026 *JINST* **21** C08022

View the article online for updates and enhancements.

You may also like

- First results on monolithic CMOS detector with internal gain
U. Follo, G. Gioachin, C. Ferrero et al.

- Simulation and first characterization of MAPS test structures with gain for timing applications
T. Corradino, C. Neubüser, G. Giovanazzi et al.

- Silicon detectors beyond LHC — RD50 status report
F. Zareef, A. Oblakowska-Mucha and T. Szumlak

This content was downloaded from IP address 130.192.92.55 on 08/10/2026 at 11:50

Published by IOP Publishing for Sissa Medialab

Received: *May 15, 2026*
Accepted: *July 27, 2026*
Published: *August 19, 2026*

21st Trento Workshop on Advanced Silicon Radiation Detectors
Perugia, Italy
17–19 February 2026

Preliminary results on the timing response of CMOS LGADs for the ALICE 3 experiment

Gaia Fabbri,[a,b,*] **M. Bregant**,[c] **S. Bufalino**,[d,e] **Z. Buthelezi**,[f] **F. Carnesecchi**,[b] **D. Cavazza**,[b] **M. Colocci**,[a,b] **T. Corradino**,[g] **M. Da Rocha Rolo**,[d] **S. Durando**,[d,h] **J. Endrizzi**,[g,i,j] **C. Ferrero**,[d] **S. Foertsch**,[f] **U. Follo**,[d,h] **G. Gioachin**,[d,e] **J. Goodhead**,[k] **M. Grenno**,[a,b] **H. Iizuka**,[l] **B. Lim**,[l] **G. Di Nicolantonio**,[m] **G. Margutti**,[m] **M. Mandurrino**,[d] **M. Masera**,[d,n] **M. Mignone**,[d] **M.G. Munhoz**,[c] **R. Nania**,[b] **F.G. Ntshangase**,[f] **V. Pagliarino**,[d,h] **L. Pancheri**,[i,j] **F. Picollo**,[d,n] **R. Ricci**,[b] **A. Rivetti**,[d] **B. Sabiu**,[a,b] **G. Scioli**,[a,b] **G.G.A. de Souza**,[c] **S. Strazzi**,[a,b] **L. Tomba**,[a,b] **S.L. Winberg**[k] **and R. Wheadon**[d]

[a] *Dipartimento di Fisica e Astronomia, Università di Bologna, Viale C. Berti Pichat 6/2, 40127 Bologna, Italy*
[b] *Istituto Nazionale di Fisica Nucleare (INFN), Sezione di Bologna, Viale C. Berti Pichat 6/2, 40127 Bologna, Italy*
[c] *Instituto de Física da Universidade de São Paulo, Rua do Matao 1371, 05508-090 Cidade Universitaria, São Paulo, Brazil*
[d] *Sezione di Torino, Istituto Nazionale di Fisica Nucleare, Via Pietro Giuria 1, 10125 Torino, Italy*
[e] *Dipartimento di Scienza Applicata e Tecnologia (DISAT), Politecnico di Torino, Corso Duca degli Abruzzi 24, 10129 Torino, Italy*
[f] *iThemba LABS, National Research Foundation, Somerset West, South Africa*
[g] *Fondazione Bruno Kessler, Via Sommarive 18, 38123 Trento, Italy*
[h] *Dipartimento di Elettronica e Telecomunicazioni (DET), Politecnico di Torino, Corso Duca degli Abruzzi 24, 10129 Torino, Italy*
[i] *Dipartimento di Ingegneria Industriale, Università di Trento, Via Sommarive 9, 38123 Trento, Italy*
[j] *TIFPA-INFN, Via Sommarive 14, 38123 Trento, Italy*
[k] *University of Cape Town, Cape Town, Western Cape, South Africa*
[l] *Center for Nuclear Study, The University of Tokyo, Tokyo, 113-0033, Japan*
[m] *LFoundry S.r.l., Via Pacinotti 7, 67051 Avezzano (AQ), Italy*
[n] *Dipartimento di Fisica, Università di Torino, Via Pietro Giuria 1, 10125 Torino, Italy*

E-mail: gaia.fabbri7@unibo.it

[*] Corresponding author.

© 2026 The Author(s). Published by IOP Publishing Ltd on behalf of Sissa Medialab. Original content from this work may be used under the terms of the Creative Commons Attribution 4.0 licence. Any further distribution of this work must maintain attribution to the author(s) and the title of the work, journal citation and DOI.

https://doi.org/10.1088/1748-0221/21/08/C08022

2026 JINST 21 C08022

Abstract: The next generation of high-energy physics experiments demands dedicated R&D to meet increasingly stringent requirements. In this context, the proposed ALICE 3 experiment at the Large Hadron Collider, scheduled to start data taking in 2036 (Run 5), aims to achieve excellent particle identification capabilities, with a dedicated silicon pixel time-of-flight detector targeting a time resolution of about 20 ps. To this end, traditional LGADs with different thicknesses have been tested, demonstrating the possibility to meet the ALICE 3 requirements for thinner sensors. However, a monolithic approach would simplify production and reduce costs by integrating the sensor and readout electronics into a single substrate. In this contribution, the main results and future outlook for the development of LGAD in CMOS technology (CMOS-LGAD) are presented. The first prototypes produced within the INFN ARCADIA project, were characterized in the laboratory using a laser source to estimate the contribution of electronic jitter to the overall time resolution; this contribution is about 40 ps, but it decreases to 22 ps in a higher power consumption configuration. Initial tests with charged particle beams have demonstrated the possibility of achieving time resolutions of 75 ps and a global efficiency larger than 95%.

Keywords: Hybrid detectors; Radiation-hard detectors; Solid state detectors; Timing detectors

2026 JINST 21 C08022

Contents

1 Introduction **1**

2 Timing performance of standard LGAD **2**
2.1 Thin LGAD 2
2.2 The double-LGAD concept 3

3 CMOS-LGAD **3**
3.1 Laser characterization 4
3.2 Charge particle characterization 5

4 Conclusions **7**

1 Introduction

The ALICE experiment at the Large Hadron Collider studies the properties of matter under extremely high energies and temperatures. The upgrade to the future ALICE 3 [1, 2] detector has been conceived by the Collaboration to address new questions, such as the thermalization and diffusion of heavy quarks, the time evolution of the Quark Gluon Plasma (QGP), and its temperature. To reach this scope, a nearly all-silicon detector based on state-of-the-art technologies has been proposed for LHC Run 5. The main improvements will focus on vertexing and tracking capabilities. In addition, excellent particle identification performance is foreseen, even at forward rapidities by means of Ring Imaging CHerenkov (RICH) and Time-Of-Flight (TOF) detectors. The latter will consist of three components: an inner layer with a radius of 19 cm and a z range from -0.62 m to 0.62 m from the interaction point; an outer layer at 85 cm with a z range from -2.79 m to 2.79 m; and two forward disks at ± 3.7 m, for a total area of about 45 m^2. The required time resolution is 20 ps to separate π/K up to 2.5 GeV/c, e/π up to 500 MeV/c and p/K up to 4 GeV/c, together with a low material budget (1–3% X_0) and radiation hardness up to 10^{13} 1 MeV n_{eq}/cm^2. An extensive R&D program on advanced silicon for timing measurements has therefore been launched. Traditional Low Gain Avalanche Detectors (LGADs) currently represent a strong backup solution, since thinner sensors with higher internal gain have demonstrated the capability to achieve 22 ps of time resolution [3], as illustrated in section 2. However, the baseline sensor technology for the ALICE 3-TOF are presently CMOS-LGADs, which integrate the sensor and readout electronics into a single monolithic substrate, thereby simplifying assembly, reducing production costs, and lowering the material budget. Recent progress in time resolution has been achieved through the production of CMOS-MAPS with internal gain. Standard LGADs and monolithic CMOS-LGADs have been tested in several test beam campaigns between 2021 and 2025 at CERN and at DESY. These measurements provide a comprehensive characterization in terms of charge collection and timing performance; moreover, the use of a telescope has enabled detailed efficiency studies of these devices.

2026 JINST 21 C08022

2 Timing performance of standard LGAD

The R&D program began with standard LGADs of varying thicknesses produced by Fondazione Bruno Kessler (FBK), which were extensively evaluated through multiple test beam campaigns. Sensors with nominal thicknesses of 25 and 35 µm and an area of $1 \times 1\,\mathrm{mm}^2$, belonging to the EXFLU0 production [4], were tested, together with devices of 15 and 20 µm thickness with an area of $1.3 \times 1.3\mathrm{mm}^2$ from the EXFLU1 production [5]. For comparison, standard 50 µm-thick LGADs from Hamamatsu Photonics K.K. (HPK) were also tested. All sensors were mounted on a V1.4-SCIPP-08/18 SantaCruz front-end board, equipped with a 2 GHz low-noise inverting trans-impedance amplifier with a trans-impedance of 470 Ω. The data were acquired in the form of waveforms using a digital oscilloscope and analyzed offline. The measurements were performed at the CERN PS T10 beamline with a beam of pions and protons at 10 GeV/c. More details on the setup and the analysis method are reported in [3].

2.1 Thin LGAD

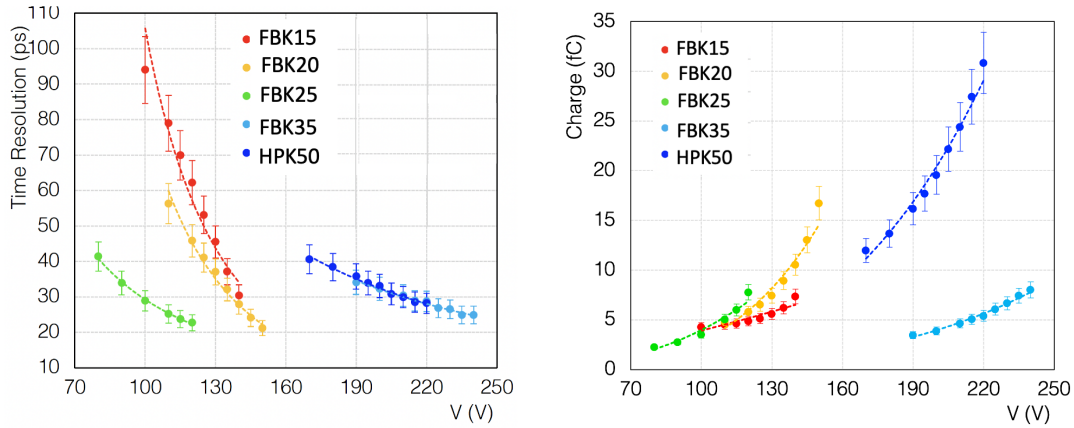

Figure 1. The time resolution at ambient temperature as a function of the voltage for sensors of different thicknesses (left); the CFD threshold for each voltage is chosen to minimize the resolution value. The charge as a function of the voltage is also shown (right). The associated uncertainties correspond to about 10% of the reported values [3].

The time resolution (left) and the deposited charge (right) of sensors with active thicknesses of 25 and 35 µm are shown in figure 1 (FBK25 and FBK35, respectively), together with those of a standard 50 µm sensor (HPK50, with an area of $1.3 \times 1.3\ \mathrm{mm}^2$), used as a reference to validate the experimental setup [3]. The time resolution of each device is extracted by independently measuring the time differences among the three sensors read out simultaneously. It is obtained as the standard deviation of a q-Gaussian fit to the time-difference distribution. A q-Gaussian function is adopted because the distributions exhibit small non-Gaussian tails, mainly originating from fluctuations in the deposited charge. The quoted time resolutions correspond to the minimum value obtained by scanning the Constant Fraction Discrimination (CFD) threshold for each sensor. The HPK50 sensor achieves a time resolution of (34 ± 3) ps at 245 V. The thinner sensors exhibit improved performance, mainly due to the reduction of Landau fluctuations associated with the smaller active thickness [6]. In particular, FBK35 reaches a time resolution of (22 ± 2) ps at 240 V, while FBK25 achieves (25 ± 3) ps at 120 V.

2026 JINST 21 C08022

Although the deposited charge is significantly lower than that of the HPK50 sensor, the thinner devices still provide better timing performance. These results indicate that, under comparable operating conditions, reducing the sensor thickness leads to an improvement in the time resolution [3]. For this reason, additional measurements were performed on even thinner prototypes with active thicknesses of 20 and 15 µm (FBK20 and FBK15, respectively). Figure 1 also reports their time resolution (left) and deposited charge (right) as a function of the applied bias voltage. Overall, the timing performance continues to improve with decreasing thickness with respect to the 50 µm reference sensor. The only exception is FBK15, whose time resolution is slightly worse than expected, likely because the front-end electronics are not optimized for the very small and fast signals delivered by such a thin sensor. This suggests that, once the contribution from Landau fluctuations is sufficiently reduced, the electronics become the dominant limitation to the overall timing performance, making the optimization of the signal-to-noise ratio increasingly important. It should be noted that FBK35 and FBK25 belong to the same production batch, whereas FBK20 and FBK15 were fabricated in a different production run. Therefore, a direct comparison of their deposited charge or operating voltage is not meaningful, since the gain characteristics differ from one production to another. Nevertheless, within each production, the deposited charge decreases with sensor thickness, as expected, while the time resolution improves for thinner sensors. All measurements were performed at ambient temperature.

2.2 The double-LGAD concept

The double LGAD (d-LGAD) concept was introduced with the aim of improving the signal-to-noise ratio (S/N) for very thin LGADs. In this configuration, two LGADs with the same nominal thickness are mounted on opposite sides of a customised PCB, and their signals are summed at the input of a common amplifier. The collected charge is expected to increase by a factor of two, enhancing the S/N and allowing the use of less power-consuming front-end electronics. Sensors with thicknesses of 15, 20, 25, 35, and 50 µm were assembled and tested, and their performance was compared to that of the two individual sensors mounted on the same board, as shown in [7]. The S/N was observed to improve by a factor between 1.3 and 2, and the time resolution improved accordingly for all the tested pairs. All the d-LGADs, including the 50 µm pair, achieved a time resolution of about 20 ps, demonstrating the effectiveness of this design in improving timing performance.

3 CMOS-LGAD

The R&D program aimed to match the requirements has continued with the introduction of LGADs in CMOS technology, which are currently considered the baseline solution in terms of sensor design. The monolithic approach offers several advantages, such as a lower material budget, reduced costs, and simplified assembly, since both the sensor and the electronics are integrated within the same substrate [8]. For this reason, to increase the signal-to-noise ratio, a p+ gain layer has been introduced beneath the collection electrode. In this context, the first prototype of the Monolithic CMOS Avalanche Detector PIXelated (MadPIX), as shown in figure 2, was developed through a collaboration between ALICE and the INFN ARCADIA project [9]. This device introduces internal gain in CMOS-MAPS fabricated by LFoundry using a 110 nm technology. The first test prototypes feature an active thickness of 48 µm and consist of 8 matrices, each containing 64 pixels, with individual pixel dimensions of $250 \times 100\ \mu m^2$. The active region is depleted by applying a bias voltage between -20 and -40 V, while the gain is controlled by a top voltage in the range of 45 to 65 V. External guard rings surround

2026 JINST 21 C08022

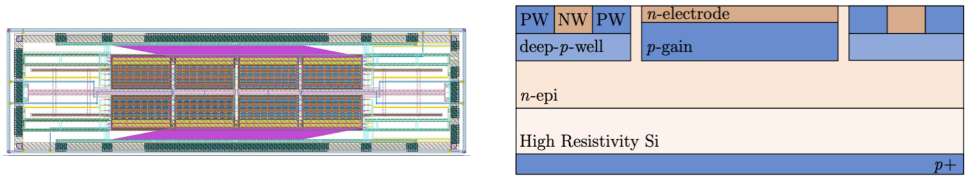

Figure 2. On the left, a schematic view of MadPIX is shown, consisting in 8 matrices, each containing 64 pixels with an area of $250 \times 100\ \mu m^2$ and an active thickness of 48 µm. On the right, a schematic representation of a pixel highlights the presence of the gain layer, beneath the collection electrode. The electric field lines at the pixel periphery do not cross the gain layer and terminate in a no-gain region, improving the timing uniformity across the pixel.

each matrix and are biased below 10 V; they collect electrons generated at the chip periphery, thus maintaining a low dark current in the pixels [8]. Outside each matrix, within the external guard rings, a 3.3 V source follower buffer is implemented. However, since all matrices share the same output, they are read out sequentially, one at a time. The front-end electronics are instead located within an $8 \times 250\ \mu m^2$ deep p-well positioned along the long side separating two pixels. The average power consumption per channel is 0.18 mW in the standard configuration, which operates at 1.2 V; however, a higher voltage configuration is also considered (1.5 V), with a consumption of 0.28 mW/ch. The first tested CMOS-LGAD prototypes belonged to the ARCADIA 3.0 Engineering Run (ER-3.0) and exhibited a lower gain, around 2–3 [8]. Nevertheless, the contribution of the gain layer to the time resolution was clearly observed. Two short-loop productions were then submitted using the same mask but with modified implantation doses or active thickness. In the first case (ER-3.1), an issue arose due to the use of an incorrect substrate, while the second (ER-3.2) enabled the fabrication of sensors with an internal gain between 11 and 14, whose performance is reported below.

3.1 Laser characterization

The first characterization step consists of identifying the operating voltages for both the top and back biases. By performing a voltage scan, it is possible to determine the voltage at which breakdown occurs (for the top bias) and punch-through is observed (for the back bias). Once the operating values are set, the electronic jitter can be estimated using a laser source with a wavelength of 1054 nm. The sensor under study is enclosed in a box internally coated with black absorbing material to prevent contamination from external light, and it is mounted on a micrometric positioning system capable of moving along the x and y directions. The laser spot is approximately 7 µm, smaller than the active region of the sensor, thus making it possible to move with high precision even within a single pixel. Thanks to a lens system, the laser intensity can be attenuated at different levels, allowing the signal amplitude to be varied accordingly. The data are collected in the form of waveforms using a digital oscilloscope.

The time resolution measurement is used to determine the contribution of the electronic jitter to the overall time resolution. The resolution was calculated as the standard deviation of a Gaussian fit performed at different percentages of the maximum signal amplitude with the CFD method, and for each amplitude, the percentage corresponding to the best time resolution was selected. The time resolution σ_t is expressed as:

$$\sigma_t^2 \simeq \sigma_{\text{TimeWalk}}^2 + \sigma_{\text{LandauNoise}}^2 + \sigma_{\text{Distortion}}^2 + \sigma_{\text{Jitter}}^2 \tag{3.1}$$

2026 JINST 21 C08022

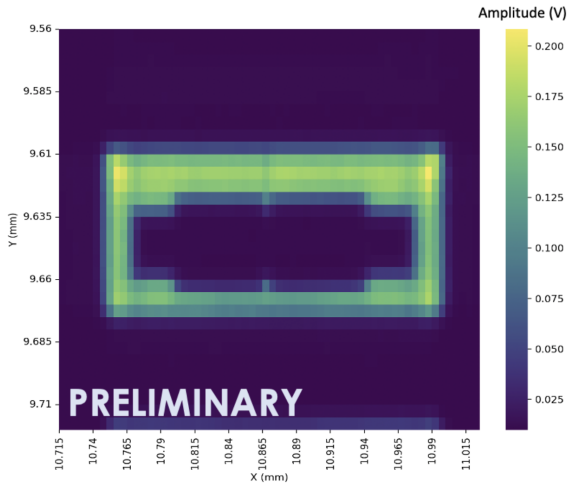

Figure 3. The signal amplitude as a function of the position in x and y. The signal is zero in the center of the pixel where the metalization is present.

where in the end only the jitter term contributes. This stems from the fact that the time walk term is corrected using the CFD method, while the distortion term is absent because the laser spot is entirely contained within the active region of the sensor. Finally, the Landau term is negligible for photons.

Figure 3 shows a pixel scan obtained by measuring the amplitude (z-axis) with the oscilloscope as a function of the x and y position. The amplitude at the centre of the pixel is zero because a metallization layer is present, while it is approximately uniform over the rest of the active area. The jitter measurement was performed in the upper central region of the sensor, where no metallization is present. The estimated electronic jitter is obtained for different signal amplitudes, corresponding to different attenuation of the photons emitted by the laser. Thanks to the lens system, the amount of light reaching the sensor is adjusted so as to reproduce the amplitude of a MIP when no attenuation was present. The electronic jitter was estimated for two different front-end electronics configurations: the standard one, with a power consumption of 0.18 mW/ch, and one in which the current flowing in the front-end was increased (0.28 mW/ch). The electronic jitter corresponding to the MIP amplitude was found to be about 40 ps for the standard configuration and 22 ps for the more power-consuming configuration, which has a higher slew rate.

3.2 Charge particle characterization

The charged-particle characterization measurements reported below were carried out during two test beam campaigns on prototypes from the ER-3.2 production. The first took place at the CERN-PS (Proton Synchrotron) using a 10 GeV/c pion/proton beam, where a cooling system based on Peltier cells and gaseous nitrogen enabled operation down to $-10\,^{\circ}C$. The second was performed at the DESY Test Beam Facility with a 4.6 GeV/c electron beam, where efficiency measurements were also conducted.

Timing performance vs temperature. At CERN-PS, thanks to a cooling system, it was possible to extract the time resolution as a function of temperature. The amplitude distributions obtained from 20 °C down to −10 °C are shown in figure 4; the amplitude shifts toward higher values as the temperature decreases, due to the increase in sensor gain. As expected, the time resolution improves

2026 JINST 21 C08022

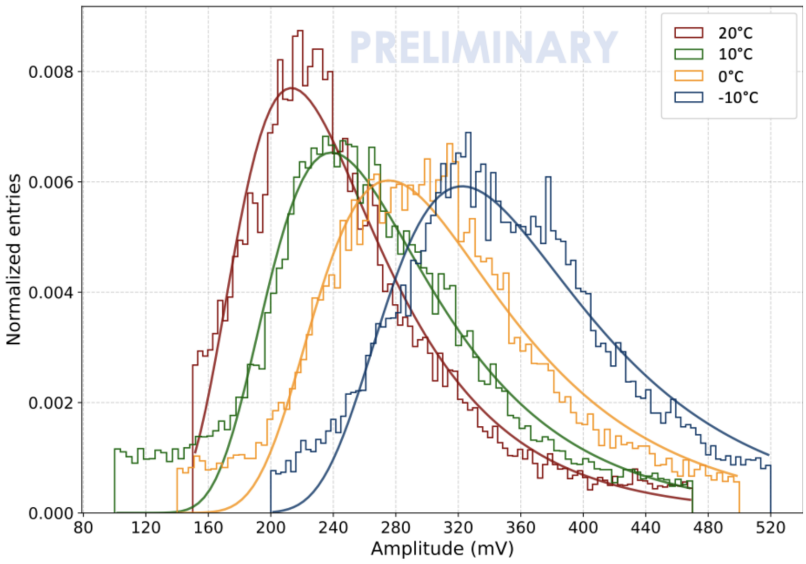

Figure 4. Amplitude distributions for different temperatures. The reported distributions were obtained at a top voltage set just below breakdown, which differs for each curve. The back voltage was fixed at -25 V.

with decreasing temperature, reaching approximately 68 ps at $-10\,^{\circ}$C, which is due to the higher amplitude of the signal. The time resolution at $20\,^{\circ}$C, the expected operating temperature of the ALICE 3-TOF detector, is instead about 75 ps. The measurements were performed by varying the top voltage for each temperature up to a value close to breakdown, while keeping the back voltage fixed at -25 V; in fact, the breakdown voltage shifts to lower values as the temperature decreases as expected.

Efficiency studies. The global and in-pixel efficiency of the tested sensor was evaluated at the DESY facility using a telescope provided by the facility itself, composed of 6 ADENIUM planes, with a telescope resolution of 4.43 µm [10]. A 50 µm LGAD was used as a trigger, and the signals were acquired with a digitizer. The acquisition was performed each time the LGAD signal exceeded a given amplitude threshold, and the acquired data were then synchronized with the telescope through the AIDA TLU and the EUDAQ2 data acquisition system [11]. Three pixels were acquired in an L-shaped configuration, belonging to the second and third columns of the matrix. In figure 5, the CMOS-LGAD global efficiency is shown as a function of the thresholds applied to the signal amplitude for a top voltage of 65 V and a back voltage of -25 V; the detection efficiency is defined as the fraction of tracks crossing the Device Under Test (DUT) area that have an associated signal within the pixel above a given threshold. The association window was set to $135 \times 60\,\mu\text{m}^2$: it was calculated as $3\sigma_{\text{telescope}} + p_{\text{pixel}}$, where $\sigma_{\text{telescope}}$ is the tracking resolution of the telescope and p_{pixel} is the pixel pitch. Since the pixel is rectangular, the association window is also rectangular. The efficiency was evaluated over a region of interest which has a diamond shape and spans adjacent pixels, including their centres. At low thresholds (below 60 mV), the amplitude distribution is dominated by the intrinsic pixel noise and by crosstalk; at this threshold, the global efficiency reaches values of about 99%.

Track reconstruction with a telescope allows to study also the in-pixel detection efficiency as a function of the particle impact position. The efficiency reaches 100% over almost the entire pixel

2026 JINST 21 C08022

surface, and no efficiency losses are observed when moving from one pixel to another along the same column (i.e. along the long side of the pixel).

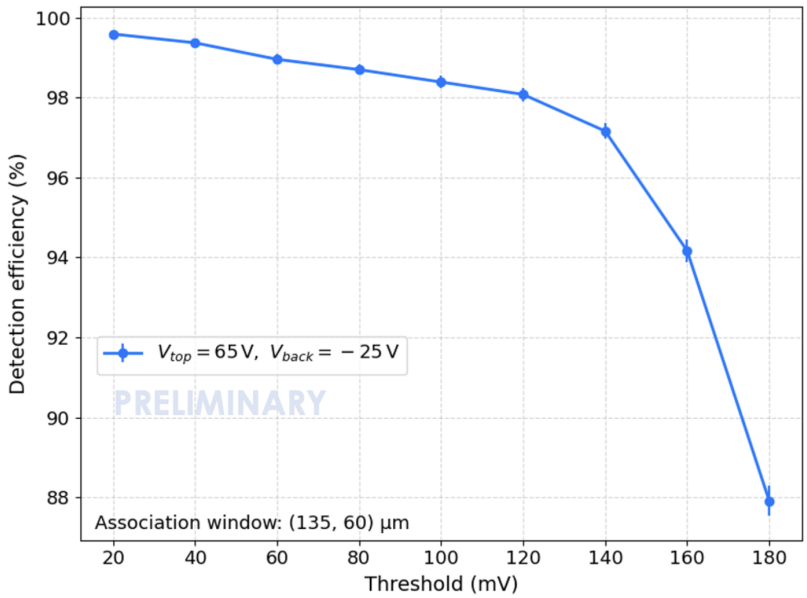

Figure 5. Global efficiency of three pixels as a function of the thresholds applied to the signal. The curve was obtained for the 0.28 mW/ch configuration at a top bias of 65 V and a back bias of −25 V.

4 Conclusions

Monolithic CMOS-LGAD prototypes represent the baseline solution for the Time-Of-Flight layers of the future ALICE 3, featuring a reduced material budget and a simplified production process. Traditional LGADs remain a solid backup solution, in particular thinner prototypes, which have demonstrated the ability to reach the 20 ps resolution required by ALICE 3. The contribution of electronic jitter to the total time resolution has been estimated using a laser source, and is about 22 ps for the best performing front-end configuration. The first CMOS-LGAD prototypes, with a thickness of 48 µm and internal gain, show a time resolution of about 75 ps at about 20 °C, the latter being the ALICE 3-TOF operating temperature and a detection efficiency above 99 %. Future developments include the characterization and testing of thinner sensors, with thicknesses down to 15 µm, which, according to simulations, are expected to meet the ALICE 3 time resolution requirements.

Acknowledgments

The FBK sensors were supported by INFN CSN5 (eXFlu project) and by the European Union's Horizon 2020 Research and Innovation Programme under Grant Agreement No. 101004761 (eXFlu-innova). The development of CMOS-LGADs was funded by the European Union's Horizon Europe programme under Grant Agreement No. 101057511. The author gratefully acknowledges the PS and DESY groups for their support during test-beam campaigns, with part of the measurements performed at the DESY Hamburg Test Beam Facility (Helmholtz Association).

2026 JINST 21 C08022

References

[1] ALICE collaboration, *Letter of intent for ALICE 3: A next-generation heavy-ion experiment at the LHC*, CERN-LHCC-2022-009 (2022) [arXiv:2211.02491].

[2] A. Dainese and A. Di Mauro, *Scoping document for the ALICE 3 detector*, CERN-LHCC-2025-002 (2025).

[3] F. Carnesecchi et al., *Beam test results of 25 and 35 μm thick FBK ultra-fast silicon detectors*, *Eur. Phys. J. Plus* **138** (2023) 99 [arXiv:2208.05717].

[4] V. Sola, *First results from thin silicon sensors for extreme fluences*, presented at the *37th RD50 Workshop*, Zagreb Online (2020).

[5] R.S. White et al., *Characterisation of the FBK EXFLU1 thin sensors with gain in a high fluence environment*, *Nucl. Instrum. Meth. A* **1068** (2024) 169798.

[6] G. Pellegrini et al., *Technology developments and first measurements of Low Gain Avalanche Detectors (LGAD) for high energy physics applications*, *Nucl. Instrum. Meth. A* **765** (2014) 12.

[7] F. Carnesecchi et al., *A new low gain avalanche diode concept: the double-LGAD*, *Eur. Phys. J. Plus* **138** (2023) 990 [arXiv:2307.14320].

[8] U. Follo et al., *First results on monolithic CMOS detector with internal gain*, 2024 *JINST* **19** P07033 [arXiv:2406.19906].

[9] M. Da Rocha Rolo et al., *ARCADIA fully depleted CMOS MAPS development with LFoundry 110 nm CIS*, *Front. Sens.* **6** (2025) 1603755.

[10] Y. Liu et al., *ADENIUM — A demonstrator for a next-generation beam telescope at DESY*, 2023 *JINST* **18** P06025 [arXiv:2301.05909].

[11] Y. Liu et al., *EUDAQ2 — A flexible data acquisition software framework for common test beams*, 2019 *JINST* **14** P10033 [arXiv:1907.10600].

2026 JINST 21 C08022